Researchers Journal of Science and Technology (REJOST)
https://rejost.com.ng

Machining Performance and Parametric Modelling for AISI 304 Steel using Biodegradable Cutting Fluid

Michael Niame Nwigbo*[1] and Nwoko-Iyeshim Apadhin[2]

Abstract

The non-biodegradability, non-recyclability and toxicity of conventional cutting fluids such as mineral oils, have raised serious concerns within the research community and prompted the renewal of research in this area with focus on replacing them with eco-friendly cutting fluids. Although several vegetable oils have been explored, there are limited work on castor oil-palm kernel oil blends that integrates physiochemical characterization, machining performance and parametric modelling for AISI 304 steel. This study evaluates the potential of using castor oil-palm kernel oil blend as green substitute for mineral oil (Aquicut 40) in metal cutting with application to turning of AISI 304 steel. Samples of castor oil, palm kernel oil, Aquicut 40 oil and formulated palm kernel-based oil were characterized by investigating the physiochemical and lubricity properties. Also, models were proposed and applied to the experimental data for validation of the results. The optimal process parameters were evaluated using Taguchi's signal-to-noise ratio. The developed oil was found to be basic (pH value: 10.10), corrosion resistant, stable, with dark yellowish coloration and generally liquid at room temperature. The application of the green oil at higher spindle speed, feed rate, and depth of cut, resulted in maximum cutting temperature (78.0°C). The optimal process parameters were achieved at lower cutting velocity and lower feed rate. The proposed models for predicting the machining parameters were suitable and reliable, with prediction accuracy above 90%. The cutting fluid promises to be environmentally friendly and safe in machining operations.

✉ Michael N. Nwigbo: nwigbon@yahoo.com

[1]Department of Mechanical Engineering, Kenule Beeson Saro-Wiwa Polytechnic, Bori, Nigeria

[2]Department of Mechanical Engineering, Rivers State University, Nigeria

Keywords: Machining, Material removal rate, Optimization, Castor oil, Cutting fluid, Wear rate

Article history
Received: November 13, 2025
Received in revised form: January 16, 2026
Accepted for publication: January 22, 2026
Available online: January 25, 2026

1.0 Introduction

The modern machining industry faces a critical sustainability crisis driven by the heavy reliance on mineral oil-based cutting fluids. While essential for reducing heat and friction, conventional lubricants pose severe environmental hazards, including soil and water pollution during disposal, and significant health risks to operators, such as skin cancer and respiratory diseases from vaporized mists (Arun *et al.*, 2023; Rajbir, 2024). Mineral oil-based fluids are typically non-biodegradable (with only 15-50% degradation) and contain toxic, carcinogenic additives (Umamaheswara *et al*., 2020). Furthermore, the rising cost of environmental compliance, coupled with the depletion of petroleum resources, has compelled industries to seek sustainable alternatives (Eze *et al*., 2021). This includes development of water-based fluids, synthetic lubricants, and more recently, eco-friendly solutions such as vegetable oils and nanofluids (Rajbir, 2024). Some of the common vegetable-based oils are cottonseed, groundnut, coconut, sesame, canola, beeswax and soybean (Saikiran and Kumar, 2019; Mariana *et al*., 2025).

The application of eco-friendly cutting fluids, offering biodegradability, lower toxicity, and renewable sourcing, in metal cutting processes have been reported by several authors (Segun *et al*., 2022; Abutu *et al*., 2023; Alaba *et al*., 2023). Dubey *et al.* (2024) noted that fluids derived from renewable, biodegradable, and non-toxic materials significantly reduce hazardous waste. Abutu *et al*. (2023) studied the impact of a mixture of mahogany seed oil and neem leaves extract on the turning of AISI 304 austenitic stainless steel, noting reductions in cutting force, feed force, thrust force, and surface roughness. Mariana *et al*. (2025) applied a mixture of castor oil and beeswax coolant to the turning of AISI 1045 steel which enhanced reduction in cutting temperature and improved surface finish – a potential substitute for synthetic oil emulsion under the same cutting conditions.

Furthermore, Awode *et al*. (2022) characterized an eco-friendly machining oil developed from neem seed oil aimed at optimizing tool wear and surface roughness during turning of AISI 304 alloy steel, and observed that the cutting fluid showed good corrosion resistance and lubricity, with improved surface finish and reduced tool wear, comparable to those of mineral oil-based oil for turning operation. Rasaq *et al.* (2024) reported reduced surface roughness and low cutting temperature with the application of hybrid palm kernel and yellow orleander oil, blended in a ratio of 1:1 in turning process of AISI 304 stainless steel.

Although several vegetable oils have been explored, there are limited work on castor oil-palm kernel oil blends that integrates physiochemical characterization, machining performance and parametric modelling for AISI 304 steel. This study addresses this gap by formulating castor oil-palm kernel oil blend for machining operations, with a view to optimize surface roughness and cutting temperature. Unlike earlier studies that focus solely on experimental performance evaluation, this study is novel in combining experimental evaluation with modelling validation for selecting sustainable cutting fluids, enhancing the decision-making process for sustainable manufacturing. The choice of combining castor oil and palm kernel oil is prompted by the high lubricity and thermal stability of castor oil with the superior flowability

(lower viscosity) of palm kernel oil, balancing out their individual limitations (Suresh *et al*., 2020).

2.0 Materials and Method

2.1 Cutting Oil Formulation

The materials used in this study include castor oil (CO), palm kernel oil (PKO) (*Elaeis guineensis*) and Aquicut 40 soluble oil. Both CO and PKO were purchased from Bori market in Nigeria and chosen due to their biodegradability and good environmental impact. To formulate the cutting oil, samples of CO and PKO were mixed with water (W) in the ratio: CO: PKO: W = 1:1:1, at room temperature to obtain 500 ml and stirred using a magnetic stirrer for 30 minutes. The flow diagram for the oil mixture is shown in Figure 1. The oils were characterized for physiochemical and lubricity properties using gas chromatography. The properties investigated include pH value, specific gravity, viscosity, flash point and pour point. The pH values of the oils were determined using a digital pH meter.

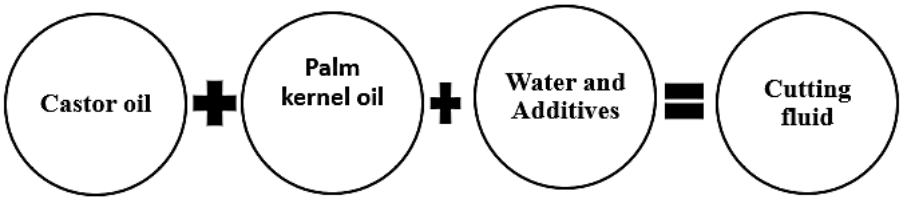

Figure 1: Palm kernel oil-based cutting fluid formulation

The determination of some of these properties was achieved using Equations (1) (Ikumapayi *et al.,* 2025).

$$\text{Specific gravity} = \frac{\text{weight of oil}}{\text{weight of an equal volume of water}} \quad (1)$$

2.2 Surface Roughness, Cutting Temperature and Morphology Measurements

The surface roughness of machined samples was determined using surface roughness tester (Surtronic 3^{+} stylus type) for cut-off length of 10 mm. Mean value of three measurements in different directions was considered as the final results for further analysis. The tester specifications were: Traverse Speed: 1 mm sec^{-1}, Display: LCD matrix, Battery: Alcaline 600. The surfaces were cleaned and positioned using a V-block before each measurement. The cutting temperature was measured using K-type thermocouple (K-316: 0 – 3000°C; ±2.5 °C or ±1%), mounted 1 mm away from the front surface and 1 mm from the upper surface of the cutting edge (Figure 2). The measurements were repeated twice for the same cutting parameters and the average results taken. The surface morphology of machined samples was examined using scanning electron microscope (SU3800).

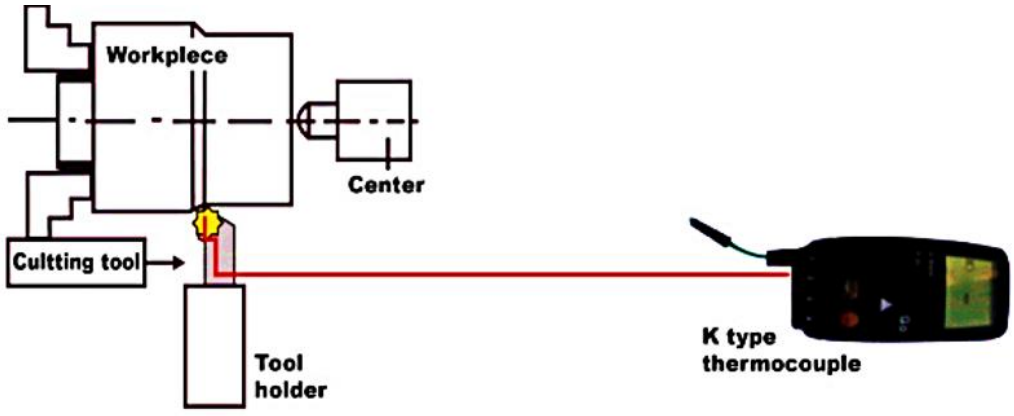

Figure 2: Schematic for cutting temperature measurement

2.3 Gas Chromatography-Mass Spectrometry Analysis

Gas Chromatography-Mass Spectrometry analysis was performed on a GCMS-3800 system (Shimadzu, Tokyo, Japan). Twenty microliters of sample were diluted to 1 ml with n-hexane (≥ 99%, Sigma–Aldrich, Germany). The column used was a 30 m × 0.25 mm inner diameter × 0.25 µL film thickness RTX-5MS column. The flow rate of helium (99.999%, AGA Lithuania) carrier gas was set at 1.23 ml/min. The oven temperature was maintained at 40 °C for 2 min after injection and then programmed at 3 °C/min to 210 °C, at which the column was maintained for 10 min. The split ratio was 1:10. The mass detector electron ionization was 70 eV. Identification of volatile compounds was carried out using a mass spectra library search (NIST 14).

2.4 Turning Procedure

The test workpiece (AISI 304 steel) having a cylindrical diameter of 80 mm, with a length of 160 mm, was turned on a three-chuck conventional lathe machine. The chemical composition and mechanical properties of AISI 304 alloy stainless steel selected are given in Table 1. To ascertain the performance of each cutting fluid sample, three cutting conditions were employed; cutting speed, depth of cut, and feed rate, as planned using the central composite design (CCD) given in Table 2. During this process, the cutting fluids were applied directly to the tool-workpiece interface at a rate of 50 ml/min. Each turning operation was done for 15 minutes. After each experiment, the insert was changed for a new one. The point of application of the cutting fluids was carefully chosen to maximize heat loss, and the rate of flow was maintained uniformly throughout the experimental procedure. The experimental setup and its schematics are shown in Figure 3. After each experiment, the machine spindle speed (v), material removal rate (MRR), and tool wear rate (TWR) were calculated using Equations (2), (3) and (4) respectively (Abutu *et al*., 2022; Kazeem *et al.*, 2023; Awode *et al*., 2022).

$$v = \pi D_o N \quad (2)$$

$$MRR = \frac{\pi f N}{4}\left(D_i^2 - D_f^2\right) \quad (3)$$

$$TWR = \frac{W_{tb} - W_{ta}}{T_m} \quad (4)$$

where, v is the cutting speed (m/min), D_o is the initial diameter before machining (mm), N is the rotational speed of the machine (rpm); f is the feed rate (mm/rev), D_f is the final diameter (mm), D_i is the initial diameter (mm); TWR is the tool wear rate (gm/min), W_{tb} is the weight of tool before machining (gm), W_{ta} is the weight of tool after machining (gm) and T_m is the total machining time (mins).

2.4 Optimization of Process Variables: Signal-to-Noise Ratio Analysis

The impact of the cutting fluid on the process parameters was evaluated using signal to noise ratio (S/N), expressed in decibel (dB) and the outcome computed as logarithmic transformation of response function, using Equations (5) and (6) based on the criteria for responses depicted in Table 3.

(i) Larger the better:

$$\text{S/N ratio} = -10\log_{10}\frac{1}{n}\sum_{i=1}^{n}\frac{1}{y_i^2} \quad (5)$$

(ii) Smaller the better:

$$\text{S/N ratio} = -10\log_{10}\sum_{i=1}^{n}\frac{y_i^2}{n} \quad (6)$$

where, n is the number of repetitions in a trial and y_i is the response value.

2.5 Modelling of Machining Parameters

The major machining parameters modelled in this study include cutting temperature and surface roughness. To achieve this, multiple regression analysis was utilized to predict the stated parameters as follows:

Model 1: Cutting temperature (CT)

$$CT = f(f_r, V, d) \quad (7)$$

where, f_r is the feed rate, V is the cutting speed and d is the depth of cut Equation (7) can be rewritten as:

$$CT = A(f_r)^n + BV + d^k \quad (8)$$

where, A and B are constant coefficients of feed rate and cutting velocity respectively and n and k are experimental constants to be obtained through analysis.

Model 2: Surface roughness (SR)

$$SR = f(v, f, d) \quad (9)$$

where, v is the spindle speed, f is the feed rate and d is the depth of cut.

Table 1: Chemical composition and Mechanical properties of AISI 304 stainless steel

Chemical Composition			Mechanical Properties		
Element	**Symbol**	**Contents (%)**	**Property**	**Value**	**Unit**
Carbon	C	0.195	Yield strength	207	MPa
Silicon	Si	0.172	Tensile strength	512	MPa
Manganese	Mn	0.389	Hardness	223	HRC
Phosphorous	P	0.034	Elastic modulus	196	GPa
Sulfur	S	0.041			
Chromium	Cr	0.304			
Molybdenum	Mo	0.018			
Nickel	Ni	0.0083			
Copper	Cu	0.100			
Vanadium	V	0.004			
Niobium	Nb	<0.0004			
Nitrogen	N	0.0083			
Boron	B	<0.0000			
Aluminum	Al	0.0106			
Tin	Sn	0.009			

Table 2: Experimental design plan

Parameters/factors	Levels		
	-1	0	$+1$
Cutting speed, x_1 (rpm)	400	600	800
Feed rate, x_2 (rpm)	0.10	0.15	0.20
Depth of cut, x_3 (mm)	0.80	1.00	1.20

Table 3: Criteria for signal-to-noise (S/N) ratio for responses

S/N	Response Name	Response Type	Unit
1	Material removal rate (MRR)	Larger the better	gm/min
2	Tool wear rate (TWR)	Smaller the better	gm/min
3	Surface roughness	Smaller the better	Ra value in microns

The model equation adopted is given by Equation (10) (Abutu *et al*., 2022).

$$SR = kf + av + d^n \quad (10)$$

where, a and k are constant coefficients of feed rate and cutting velocity respectively and n is an experimental constant to be obtained through analysis. Equation (10) can be rewritten as:

$$\ln(SR) = \ln(k) + \ln(f) + \ln(a) + \ln(v) + n\ln(d) \quad (11)$$

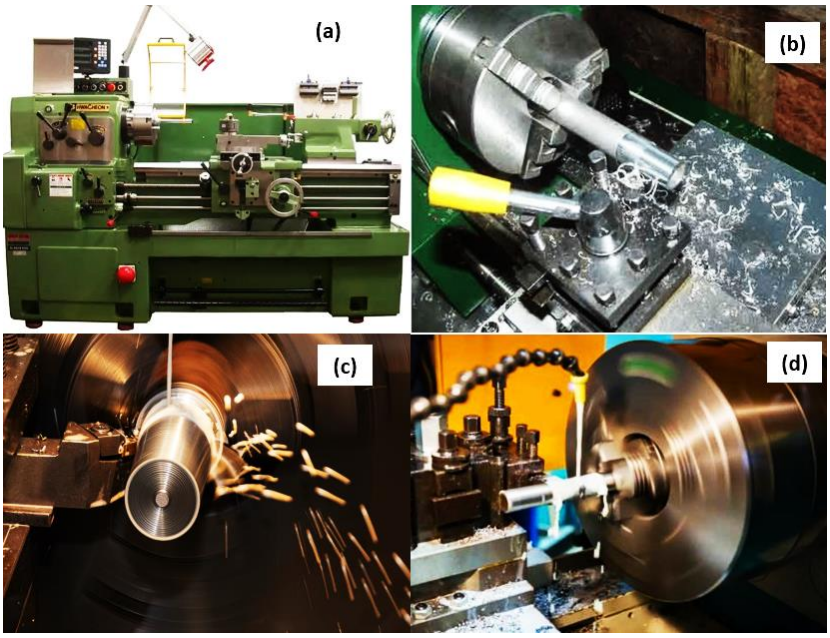

(a) Lathe machine (b) Dry turning (c) Turing with CO/PKO oil (d) Turning with A40S oil

Figure 3: Turning operation

2.6 Analysis of Variance and Error of Prediction

Analysis of variance (ANOVA) which comprises the degree of freedom (DOF), sum of square (SS), mean square (MS), f-value (F) and percentage contribution (P) was conducted on the experimental results in order to study the percentage contributions of machining parameters on the performance of cutting fluids. A confidence level of 95% and significance level of 5% was adopted for analysis. Also, the total sum of for all ANOVAs was calculated using Equation (12) (Awode *et al*., 2022).

$$SS_{Total} = \sum_{i=1}^{n} y_i^2 - \frac{1}{n}(y_i)^2 \quad i = 1,2,3,\dots n \qquad (12)$$

where, SS is the sum of square, n is the number of observation and y is the observations in ith sample. The deviation of model prediction from the corresponding experimental result, referred to as error of prediction (ε) or deviation was obtained using Equation (13) (Jodar and Franco, 2025).

$$\varepsilon = \left(\frac{E_p - M_p}{E_p}\right) \text{x } 100\% \qquad (13)$$

where, E_p and M_p are the experimental and model-predicted parameters respectively.

3.0 Results and Discussion

The physiochemical properties of the oil samples used during the turning operations are given in Table 4. The castor oil, palm kernel oil, castor oil/palm kernel oil blend and Aquicut 40 soluble cutting oil were yellow, dark yellow, dark yellow and milky white respectively in color, and generally liquid at room temperature. The measured parameters have close values to those recorded in the literature (Abutu *et al*., 2022; Eze *et al*., 2021; Segun *et al*., 2022).

The lubricating properties of the sampled cutting fluids presented in Table 4 revealed higher flash points for commercial oil (Aquicut 40) and the formulated castor oil/palm kernel oil compared with those of castor oil (251) and palm kernel oil (229ºC). According to Alaba *et al*. (2023) and Egbuna *et al*. (2021), the flash points of palm kernel oil were respectively 220ºC and 223ºC. The higher flash point of the developed oil in this study implies greater fire safety and suitability for high-temperature applications, reducing smoke/fire risk (Alaba *et al*., 2023). The specific gravity values for palm kernel oil, castor oil and castor oil/palm

kernel oil obtained in this study was found to be close to those obtained for African pear seed oil (0.917) by Eziwhuo *et al*. (2019), palm kernel oil (0.907) by Alaba *et al.* (2023), castor oil (0.86) by Eze *et al*. (2021), and seed oil (0.919) by Awode *et al*. (2022).

The pH values of all the cutting fluid samples were in alkaline state (greater than 7.0) which indicates that they will not corrode metal during machining processes while the viscosity value of greater than 1.9 Pas at 28°C signified the measure of fluid friction, as a result represent a good internal resistance of the oil to flow, due to the thick film formation and rolling action of the vegetable oil blend comparable with A40S. The pH value is similar to what was reported by Alaba *et al*. (2023), during an MQL turning operation of AISI 1039 steel, though slightly lower than the results of this study. The disparity between the oil pH found in this study and those in literature might be related to genetic variances, climate, plant species, soil conditions, and inappropriate processing methods including exposing harvested seeds to sunlight for an extended period, which has the potential to significantly reduce or increase pH. Also, all the cutting oils exist as liquids at room temperature, except that palm kernel oil begins to solidify at temperatures slightly less than room temperature but will liquefy when exposed to sunlight or subjected to heat. Based on these results, the castor/palm kernel oil extracts can be adopted in the preparation of the vegetable oil cutting fluids.

Table 4: Physiochemical and lubricity properties of cutting oil used

S/N	Property	CO	PKO	CO/PKO	A40S
1	Corrosion Level	Corrosion resistant	Corrosion resistant	Corrosion resistant	Corrosion resistant
2	Viscosity at 28°C (Pas)	1.9449	2.53	2.023	2.098
3	pH value at 30% oil content	8.50	10.32	10.10	9.60
4	Stability	Stable	Stable	Stable	Stable
5	Color	Yellow	Dark yellow	Dark yellow	Milky white
6	Specific gravity	0.9784	0.9180	0.9010	0.9012
7	Density(g/cm^3) at 28°C	0.9955	0.9043	0.8954	0.9930
8	Pour point (°C)	27	20.7	18.7	19.6
9	Flash point (°C)	251	229	252.3	254
10	Appearance at 28°C	Liquid	Liquid	Liquid	Amber liquid

CO: Castor oil PKO: Palm kernel oil
CO/PKO: Castor oil/ Palm kernel oil A40S: Aquicut 40 soluble cutting oil

3.1 Gas Chromatograph (GC) Analysis of Cutting Fluids

The chromatogram and data of fatty acids composition of castor oil and palm kernel oil presented in Table 5 and Figure 4 respectively reveal that the most abundant fatty acids for castor oil and palm kernel oil were linoleinic acid (90.00%) and lauric acid (42.21%) respectively. This result also indicates significantly high amount of unsaturated fatty acid content (96.30%) and lower

value of saturated fatty acid (3.70%) in castor oil. Conversely, palm kernel oil presented high amount of saturated acid (68.39%) and lower value of unsaturated fatty acid (31.41%). Generally, fatty acids have been reported to significantly improve lubrication by forming strong, protective boundary films on metal surfaces, reducing friction and wear, especially in bio-lubricants, due to their polar head and long non-polar chains that adhere to metal, with unsaturated acids often enhancing film stability and longer chains providing stronger interactions, though high temperatures can limit performance (Alaba *et al.*, 2023; Abutu *et al.*, 2023). They act as anti-wear additives and friction modifiers by creating a tribo-layer that prevents direct metal-to-metal contact, making systems run smoother and last longer. This suggests that a blend of castor oil and palm kernel oil will serve as a good cutting fluid.

Table 5: Fatty acid composition of vegetable oils

S/N	Fatty acids	Composition (%)		
		CO	PKO	CO/PKO
1	Capric acid	-	0.43	0.27
2	Lauric acid	-	42.21	37.80
3	Myristic acid	-	11.34	10.91
4	Palmitic acid	0.81	9.07	6.95
5	Palmitoleic acid	-	5.22	5.06
6	Stearic acid	0.94	5.34	4.78
7	Oleic acid	2.80	17.76	17.02
8	Linoleic acid	4.10	4.93	4.33
9	Linolenic acid	0.97	3.50	2.95
10	Ricinoleic acid	90.00	-	75.81
11	Eicosanoic acid	0.30	0.12	0.11
11	Others	0.9	0.08	0.63
12	Saturated fatty acid	3.70	68.39	55.23
13	Unsaturated fatty acid	96.30	31.41	78.39

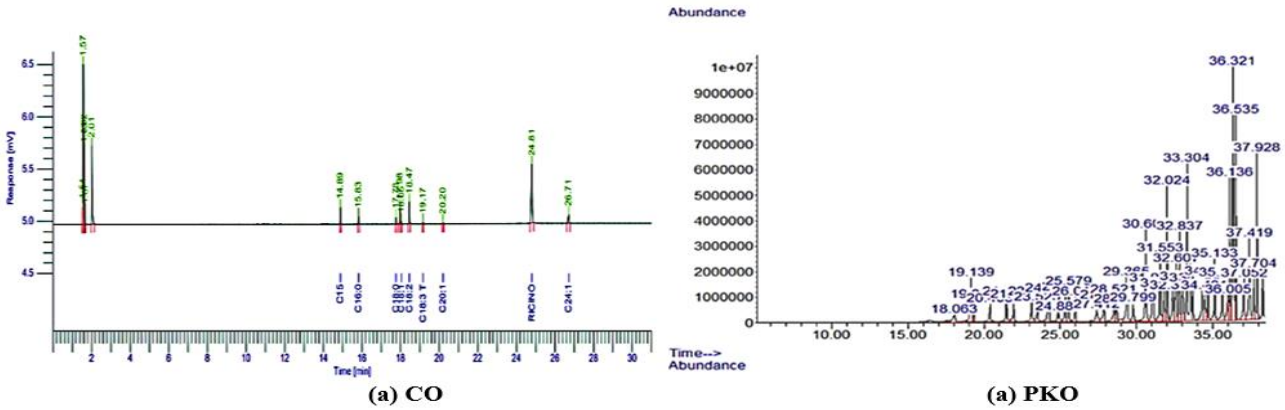

(a) CO (a) PKO

Figure 4: Gas Chromatograms of oils

3.2 Machined Surface Morphology

The scanning electron micrograph (SEM) micrographs given in Figure 5 reveals the effect of cutting fluids and cutting speed on machined surfaces compared with dry cutting condition. The as-received AISI 304 steel consisted of equiaxed, twinned austenitic-grain structure, with dark patches which are traces of alloying elements indicative of chromium coating on the surface and grain boundaries of the samples, typical of AISI 304 austenitic stainless steels. However, dry machined surfaces at low cutting speeds (400 rpm) showed cavities, metal debris and feed marks with smeared material particles, which may be due to the increased rubbing action of abrasive grits with work material. Surfaces machined with cutting fluid (wet turning), do not contain cavities nor metal debris, but they show evidence of material side flow, mainly due to very smooth interaction of grit over workpiece during grinding. Similar effects were reported by other authors during machining of modified AISI 420 stainless steel (Segun *et al*., 2022).

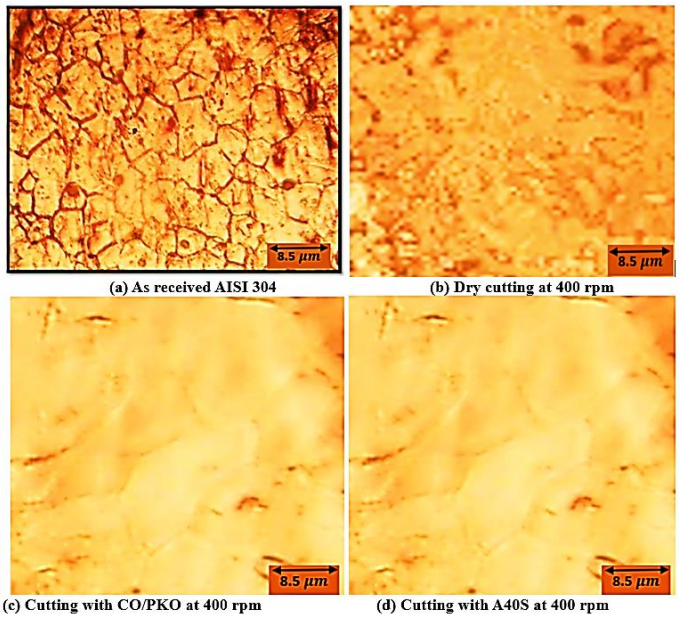

Figure 5: SEM micrographs of machined surfaces (x 400)

3.3 Cutting Temperature

The effect of the application of the various oils on cutting temperature under varying conditions of spindle speed and depth of cut is presented in Table 6. Generally, lower cutting temperatures were observed with lower cutting speed and depth of cut, indicating less heat dissipation on the cutting fluid from the abrasive effect that exists between the cutting tool and the workpiece (Arifuddin *et al*., 2022). The cutting temperatures reduced significantly with the application of the cutting oils compared with dry cutting, with maximum cooling effect noticeable with the use of CO/PKO blend. This could be attributed to the lubricity obtained in CO/PKO blend because of its sulfur content and heat dissipation ability at a faster rate when compared to Aquicut 40 oil (Segun *et al.,* 2022). Furthermore, the good thermal properties such as high flash point, fire point and high viscosity contribute to the excellent lubricity of the vegetable oil blend. Evidently, the use of blended vegetable oil-based coolant reduces the impact of rubbing abrasive grits with workpiece by forming a thin film of lubrication layer and reduce the wear of micro abrasives by dulling (Seresh *et al.,* 2020). The material removal

rates were also observed to be constant at varying cutting speed, due to inversely adjusting the feed rate or depth of cut. This approach has significant implications for tool life, surface quality, and energy consumption (Ucheonwu *et* al., 2025). It often leads to reduced tool-chip contact time and lower cutting forces, resulting in longer tool life and less tool wear, reduced heat generation, leading to a smoother finish.

3.4 Optimization of Process Parameters

The SN values of surface roughness (finish) values for the machined steel samples were calculated (in decibel scale (dB)) as logarithmic transformation of surface roughness function and presented in Table 7.

Table 6: Cutting temperature

v (rpm)	d (mm)	Material Removal Rate (mm^3/min)					Cutting Temperature (^oC)				
		DC	PKO	CO	A40S	C-P	DC	PKO	CO	A40S	C-P
400	1.00	3017.1	3017.1	3017.1	3017.1	3017.1	39.0	36.2	34.5	32.0	30.0
400	1.20	5385.6	5385.6	5385.6	5385.6	5385.6	62.4	52.5	57.1	36.7	32.1
400	0.80	4867.7	4867.7	4867.7	4867.7	4867.7	68.2	51.5	54.0	48.2	53.7
600	0.80	3650.7	3650.7	3650.7	3650.7	3650.7	55.4	43.4	46.9	40.1	39.4
600	1.00	6788.6	6788.6	6788.6	6788.6	6788.6	60.1	45.5	50.0	41.0	43.1
600	1.20	10771.2	10771.2	10771.2	10771.2	10771.2	63.7	38.9	42.6	35.2	38.3
800	0.80	4857.7	4857.7	4857.7	4857.7	4857.7	60.6	48.2	52.5	56.2	59.0
800	1.00	9051.4	9051.4	9051.4	9051.4	9051.4	64.3	59.2	63.8	69.4	70.5
800	1.20	14361.6	14361.6	14361.6	14361.6	14361.6	67.0	66.4	68.9	78.0	81.0

v: Cutting speed d: Depth of cut DC: Dry cutting C-P: Castor oil-palm kernel oil blend

Table 7: Optimal surface roughness analysis

Order	f	d	Surface Roughness (μm)					SN Ratio (dB)					OCF
	(mm/rev)	(mm)	DC	CO	PKO	CO/PKO	A40S	DC	CO	PKO	CO/PKO	A40S	
1	0.10	1.00	0.902	0.466	0.509	0.220	0.211	5.667	11.404	10.705	19.011	18.286	CO/PKO
2	0.15	1.20	1.054	0.507	0.625	0.561	0.545	4.315	10.671	8.854	10.220	10.043	
3	0.20	0.80	1.205	0.622	0.689	0.601	0.599	3.152	8.895	8.007	9.524	9.223	
4	0.10	0.80	0.625	0.899	0.753	0.691	0.677	8.853	5.696	7.235	8.622	8.159	CO/PKO
5	0.15	1.00	0.722	0.787	0.835	0.877	0.868	7.601	6.852	6.338	7.101	6.001	
6	0.20	1.20	0.903	0.995	1.033	1.200	1.100	5.658	4.815	4.489	3.951	3.943	
7	0.10	0.80	0.766	0.607	0.674	0.572	0.568	7.087	9.107	8.198	9.788	9.684	CO/PKO
8	0.15	1.00	0.900	0.697	0.755	0.710	0.600	5.686	7.907	7.212	9.462	9.201	
9	0.20	1.20	1.106	0.807	0.856	0.695	0.693	3.188	6.634	6.122	8.200	7.957	

DC: Dry cutting PKO: Palm kernel oil CO: Castor oil f: Feed rate OCF: Optimal cutting fluid

d: Depth of cut A40S: Aquicut 40 oil CO/PKO: Castor oil/Palm kernel oil

It is also observed, that both feed rate and depth of cut have significant effect on the response (surface roughness) at varying spindle speed. Regardless of the category of the quality characteristic, a higher SN ratio corresponds to better quality characteristic indicating the optimal

level of the process parameters. Based on the solution analysis in Table 7, the optimal values of input process parameters were achieved with palm kernel/castor oil turning with cutting velocity (400 rev/min), feed rate (0.10 mm/rev) and depth of cut (1.0 mm). This directly translates to more accurate and reliable measurements of the surface roughness parameters, suggesting that the castor oil-palm kernel oil blend can serve as a substitute for commercial cutting fluid in machining operations.

3.5 Model Predictions

The spindle speed (v), feed rate (f), and depth of cut (d), were used to develop a multiple regression model with a 95 percent confidence level for the process responses (surface roughness (Ra) and cutting temperature (CT)). The value of the model's determination coefficients was calculated to assess the model's suitability (R^2). The relevance of the model increases as the R^2 value increases, that is, when it approaches one. Based on the experimental results, Equations (14) and (15) present the mathematical models for surface roughness and cutting temperature respectively, together with their R^2 values. The derived models revealed significantly aligned and similar trends of data point distribution, but varying magnitudes of experimental and model-predicted results could be observed as shown in Table 8. The implication of the disparity in these magnitudes is that the model predictions deviated from the corresponding experimental results. This was attributed to non-consideration and non-inclusion (to the core model structure) responses from the physicochemical interactions between the formulated cutting oil and the cutting parameters (spindle speed, feed rate and depth of cut), as well as the surface properties of the material during turning operation. These responses on the other hand, play very vital roles during the experiment and so affected the results of the investigation. Equation (14) indicates that all three parameters (v, f, d) have positive coefficients, meaning that an increase in any of these parameters will lead to an increase in predicted surface roughness (a rougher surface). The coefficient for f (2.46) is significantly higher than the others, indicating that the feed rate is the most influential factor on surface roughness in this specific model. The extremely small coefficient for v (0.0000242) suggests that cutting speed has a very minimal impact on Ra in this particular experimental setup.

$$Ra\ (Ra\ (\mu m) = -4.84 + 0.0000242v + 2.46f + 0.182d \quad (14)$$

Model summary: $R^2 = 47.46\%$

$$CT\ (℃) = -27 + 0.287v + 319f - 60d - 0.000240v^2 - 1160f^2 + 37d^2 + 8fd \quad (15)$$

Model summary: $R^2 = 77.73\%$

Table 8: Comparison of experimental and model-predicted surface roughness and temperature

v (rpm)	d (mm)	f (mm/rev)	Surface Roughness (μm)			Cutting Temperature (℃)		
			ER	MPR	Deviation (%)	ER	MPR	Deviation (%)
400	1.00	0.10	0.211	0.228	8.05	30.0	32.1	7.00
400	1.20	0.15	0.408	0.380	- 6.86	32.1	32.8	2.33
400	0.80	0.20	0.586	0.570	- 2.73	53.7	54.9	2.23
600	0.80	0.10	0.643	0.671	4.36	39.4	38.1	- 3.30
600	1.00	0.15	0.704	0.730	3.69	43.1	44.6	3.48
600	1.20	0.20	1.000	1.090	9.00	38.3	40.1	4.70
800	0.80	0.10	0.468	0.502	7.27	59.0	60.3	2.20
800	1.00	0.15	0.577	0.603	4.51	70.5	71.4	1.28
800	1.20	0.20	0.643	0.675	4.98	81.0	82.2	1.48

v: Spindle speed f: Feed rate d: Depth of cut ER: Experimental results MPR: Model predicted results

The analysis of variance (ANOVA) analysis for surface finish and cutting temperature, using the vegetable oil blend at 800 rpm cutting speed is given in Table 9. The results show that the models and the input parameters are significant, with p-values less than 0.0001. Evaluation of the models reveal that the model is statistically relevant in explaining the relationship between the dependent variables (surface finish and cutting temperature) and independent variables (spindle speed, depth of cut and feed rate). However, the model accounts for 90 % of the experimental data, an indication that little errors or deviations (which are less than 10 %) are observed between the theoretical and actual cutting temperatures of the steel samples.

Table 9: ANOVA analysis for surface roughness and cutting temperature using CO/PKO at 800 rpm

	Surace Roughness					Cutting Temperature				
Source	**df**	**SS**	**MS**	**F**	**P (%)**	**df**	**SS**	**MS**	**F**	**P (%)**
v	2	23.35	11.68	23.78	41.25	2	0.01490	0.007448	0.63	16.00
f	2	27.99	14.00	28.50	49.44	2	0.03233	0.016165	1.36	35.50
d	2	4.29	2.14	4.37	7.57	2	0.02278	0.011390	0.96	24.30
Error	2	0.98	0.49		1.73	2	0.02382	0.011911		24.20
Total	8	56.61	28.31		100.00	8	0.09383			100.00

v: Cutting speed ***f***: Feed rate ***d***: Depth of cut df: Degree of freedom
SS: Sum of squares MS: Mean sum of squares F: Fisher's value P: Percentage contribution

Figure 6 shows the surface plots for the interactions of cutting speed and depth of cut on the tool-workpiece interface temperature for each cooling medium, dry cutting, A40S cutting, and CO/PKO cutting, respectively. For dry cutting (Figure 6a), there is an increase in the temperature developed within the cutting tool-workpiece interface similar to the observation of Segun *et al.* (2022). The increase in temperature could be at tributed to the bulk of cutting chips formed around the cutting tool and workpiece. Also, stress concentration and plastic deformation of the material could be responsible for this increase in temperature. The lack of cooling media such as fluid or pressurized air also contributed to the high temperature observed in this condition (Segun *et al.*, 2022). Similar trend is observed the A40S cutting (Figure 6b) except that lower temperatures are recorded in the cutting tool-workpiece interface. This temperature reduction could be attributed to a cooling medium and rapid transportation of chips from the cutting region, and also agrees with the findings of Rasaq *et al.* (2024).

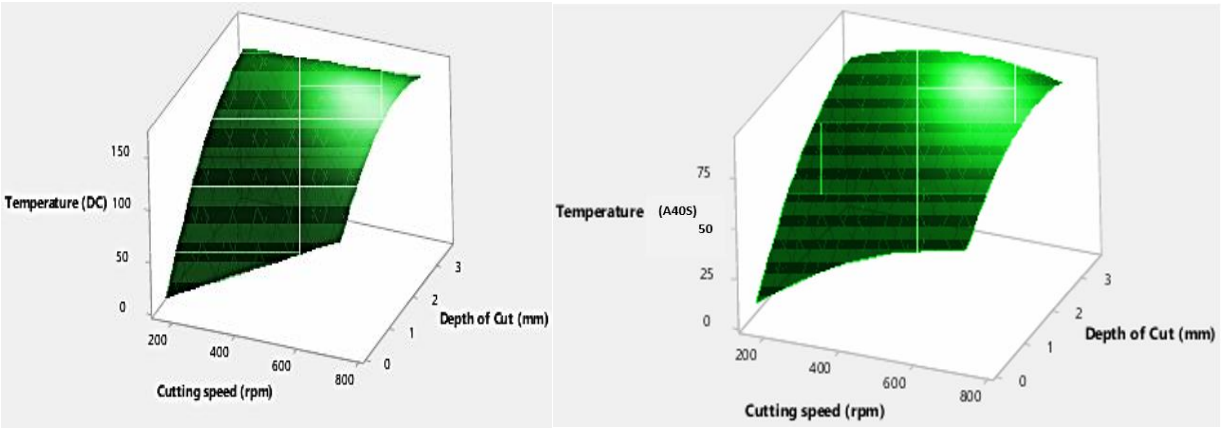

(a) Dry cutting condition (b) A40S cutting condition

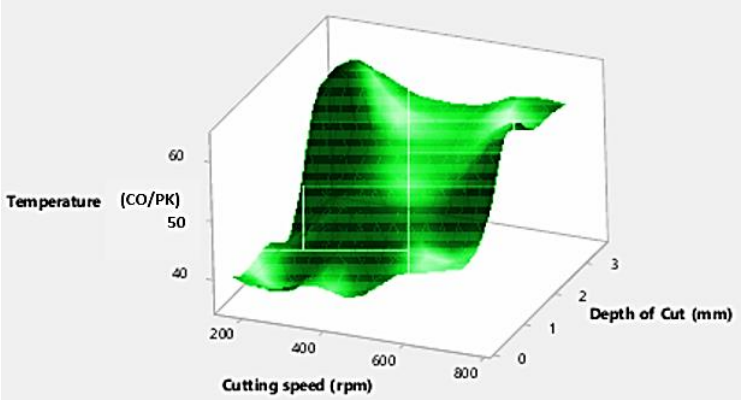

(c) CO/PKO cutting condition

Figure 6: Surface plot for the interactions of process parameters

The trends observed in Figure 6(c) show lower temperatures at the cutting tool-workpiece interface than other cooling mediums used as cutting depth increases. However, a gentle slope was observed as cutting speed increases with an increase in cutting tool-workpiece temperature. This suggests that the surface roughness has low sensitivity to changes in the input machining parameters (cutting speed, feed rate, and depth of cut), implying a robust and stable machining process.

4.0 Conclusion

This study promotes the adoption of environmentally sustainable practices by endorsing the use of a novel biodegradable vegetable oil (castor oil-palm kernel oil blend) as cutting fluid for machining processes, thus contribute to the overall field of machining science. The following conclusions can be drawn, based on the results obtained:

(a) The fatty acid composition and physiochemical properties of the developed oil were consistent with the various existing oils reported in literature. Consequently, the feasibility of using castor oil-palm kernel oil blend as a substitute for mineral-based oils in cutting fluid formulation is affirmed.

(b) The performance of the developed cutting fluid in terms of stability, corrosion resistant, pH and viscosity compared favorably with A40S. As a result, it is environmentally friendly as it is safe for use in machining operations.

(c) Generally, cutting speed and depth of cut are attributed to the increase in cutting tool temperature.

(d) The proposed models for predicting the machining parameters were suitable and reliable, with prediction accuracy above 90%.

(e) It is recommended that further research be done to enhance the ability of green cutting fluids and also evaluate the type of tool wear when a castor oil/palm kernel oil-based cutting fluid is used.

References

Abutu, J., Elachi, E. E., Tanko, B., Akene, P., Musa, K. & Lawal, S. A. (2023). Development of cutting fluid from mahogany seed oil and neem leaves for the turning of AISI 304 austenitic stainless steel. *Journal of Materials and Environmental Science*, 14 (8): 878 – 889.

Abutu, J., Oluleye, M. A., Okechukwu, C. Salawu, S. I., Dame, B. & Unamba, K. U. (2022). Performance assessment of vegetable oil-based cutting fluid developed from palm kernel oil using multi-response optimisation technique. *Nigerian Journal of Technology,* 41 (1): 99 –113.

Alaba, E. S., Kazeem, R. A. Adebayo, A. S. Petinrin, M. O. Ikumapayi, O. M., Jen, T. C. & Akinlabi, E. T. (2023). Evaluation of palm kernel oil as cutting lubricant in turning AISI 1039 steel using Taguchi-grey relational analysis optimization technique. *Advances in Industrial and Manufacturing Engineering*, 6 (2023): 100115.

Arifuddin, A., Redhwan, A. A., Syafiq, A. M., Zainal, A., S., Aminullah, A. R. & Azmi, W. H. (2022). Effectiveness of hybrid Al_2O_3-TiO_2 nano cutting fluids application in CNC turning process. *Archives of Materials Science and Engineering*, 117 (2): 70 – 78.

Arun, K. K., Ramesh, Chandra, M. & Aditya, K. (2023). The role of bio-based cutting fluids for sustainable manufacturing and machining processes: A holistic review. *Mechanical Engineering for Society and Industry*, 3 (3): 166-180.

Awode, E. I., Lawal, S. A., Olaiya, K. A. & Abutu, J. (2022). Characterization of eco-friendly cutting fluid developed from neem seed oil. *Nigerian Journal of Technology*, 41 (4): 700 –711.

Dubey, Y., Sharma, P., Singh, M. P., Rao, G. S., Mohammad, Q., Lakhanpal, S., & Rao, A. L. N. (2024). A review on green machining: Environmental and economic impacts of cutting fluids. *E3S Web of Conferences*, 505: 01030.

Eze, O. C., Owuama, K. C. & Okafor, O. C. (2021). Performance evaluation of castor oil and neem oil as cutting fluids applied in drilling operation of mild steel. *World Journal of Engineering Research and Technology*, 7 (4), 90 – 111.

Ikumapayi, O. M., Laseinde, O. T., Kazeem, R. A., Onu, P. & Ting, T. T. (2025). The development and performance assessment of palm kernel nut oil as a cutting fluid for the turning of AA6061. *Lubricants*, 13: 279.

Jodar, J. & Franco, P. (2025). Equivalent error-based modelling for prediction and analysis of measuring accuracy in 3-axis FXYZ coordinate measuring machines from position, repeatability and reversibility errors. *International Journal of Precision Engineering and Manufacturing*, 26: 67–80.

Kazeem, R. A. Enobun, I. O. Akande, I. G. Jen, T. C. Akinlabi, S. A. Ikumapayi, O. M. & Akinlabi, E. T. (2023). Evaluation of palm kernel oil as lubricants in cylindrical turning of AISI 304 austenitic stainless steel using Taguchi-grey relational methodology. *Materials Research Express*, 10 (2023): 126505.

Mariana, A. G., Lucas, B., Roberto, G. P. & Juan, M. P. (2025). The use of castor oil and beeswax as biodegradables cutting fluids on turning of AISI 1045 steel. *Materials and Manufacturing Processes*, 40 (5): 689-701.

Rajbir, S. R. (2024). Review of cutting fluid technologies in machining processes. *International Journal of Engineering Research and Development*, 20 (11): 1450 – 1454.

Rasaq, K., Tien-Chien, J., Godwin, A., Stephen, A. & Esther, A. (2024). Performance evaluation of hybrid biodegradable oils as a lubricant during cylindrical turning of AISI 304 austenitic stainless steel. *AIMS Materials Science*, 11(2): 256–294.

Saikiran, M. and Kumar, P. (2019). An investigation on the effects of vegetable oil-based cutting fluids in the machining of

copper alloys. *Materials Today Proceedings*, 19: 455–461.

Segun, M. A., Bright, K. O. & Peter, O. O. (2022). Performance evaluation of coconut oil-based cutting fluid with biodegradable additives on cylindrical turning of AISI 1040 carbon steel. *Acta Metallurgica Slovaca*, 28 (1): 10 – 13.

Suresh, K., Karthikeyan, S. & Ravikumar, K. (2020). Lubrication performance of castor oil blended with other vegetable oils in grinding of Inconel 625. *IOP Conf. Series: Materials Science and Engineering*, 923: 012027.

Ucheonwu, P. H. H., Sada, S. O., Enyi, L. C., Sinebe, J. E. & Ekpu, M. (2025). Effect of cutting speed, depth of cut, and feed rate on metal removal rate in the machining of a cylindrical mild steel bar. *Journal of Applied Sciences and Environmental Management*, 29 (3): 1011-1013.

Umamaheswara, R.R.S., Satyanarayana, G., Anil, P. M. & Subba, R. (2020). Wear characteristics of alternative, bio-degradable cutting fluids. *Materials Today*, 26(2):1352-1355.